

UNCLASSIFIED

AD NUMBER

AD324812

CLASSIFICATION CHANGES

TO: unclassified

FROM: restricted

LIMITATION CHANGES

TO:

Approved for public release, distribution unlimited

FROM:

Distribution authorized to U.S. Gov't. agencies only; Foreign Gov't. Info.; 7 Apr 1961. Other requests shall be referred to the British Embassy, 3100 Massachusetts Ave., NW, Washington, DC 20008.

AUTHORITY

British Embassy, per DTIC Form 55, dtd Mar 11, 2003; British Embassy, per DTIC Form 55, dtd Mar 11, 2003

THIS PAGE IS UNCLASSIFIED

CONFIDENTIAL

MODIFIED HANDLING AUTHORIZED

AD 324 812 L

*Reproduced
by the*

ARMED SERVICES TECHNICAL INFORMATION AGENCY
ARLINGTON HALL STATION
ARLINGTON 12, VIRGINIA



CONFIDENTIAL
MODIFIED HANDLING AUTHORIZED

NOTICE: When government or other drawings, specifications or other data are used for any purpose other than in connection with a definitely related government procurement operation, the U. S. Government thereby incurs no responsibility, nor any obligation whatsoever; and the fact that the Government may have formulated, furnished, or in any way supplied the said drawings, specifications, or other data is not to be regarded by implication or otherwise as in any manner licensing the holder or any other person or corporation, or conveying any rights or permission to manufacture, use or sell any patented invention that may in any way be related thereto.

Page/s
missing from
original document.

FIG. 6

RESTRICTED

P.T.P. (R) 35

P.T.P. (R) 35

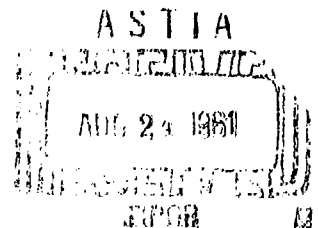
NOX

CHEMICAL DEFENCE EXPERIMENTAL ESTABLISHMENT

ADHESION OF SPHERICAL PARTICLES
TO PLANE SURFACES

BY

N.L. CROSS AND H. STRETCH



PORTON TECHNICAL PAPER No. (R) 35

C.D.E.E.

Porton

Wilts.

RESTRICTED

48202
CATALOGUED BY ASTIA
AS AD NO.

RESTRICTED

U. S. CONFIDENTIAL
MODIFIED HANDLING AUTHORIZED

PORTON TECHNICAL PAPER NO. (R) 35

DATE 7th April, 1961.

ADHESION OF SPHERICAL PARTICLES TO PLANE SURFACES

by

N.L. Cross and H. Stretch

SUMMARY

1. The adhesion of spherical particles to plane glass and quartz surfaces has been investigated under various humidity conditions, and compared with the results obtained using similar spheres made radioactive by the incorporation of traces of active europium isotopes.

2. Much stronger adhesion is found with active specimens than with inactive ones when examined in water vapour atmospheres of up to 61% R.H. The values obtained with active particles may be expressed in the empirical form

$$Z = k\epsilon^{-sR}$$

in which Z is the adhesion force of a sphere of radius R , k a parameter concerned with the dielectric constants of the surfaces in contact, and s with the humidity effect, i.e. change in the conductance of the surfaces in consequence of moisture deposition.

3. In atmospheres of near saturation humidity, the radioactive effect is replaced by the even stronger adhesion produced by surface tension forces.

4. A more exact theoretical treatment is offered of the adhesion of an inactive spherical particle to a plane surface than has been previously available.

(Sgd.) H.L. Green,
Supt., Physics Research Division.

NLC/HS/RT

(Sgd.) A.S.G. Hill,
Deputy Director.

U. S. CONFIDENTIAL
MODIFIED HANDLING AUTHORIZED
RESTRICTED

PORTON TECHNICAL PAPER NO. (R) 35

DATE: 7th April, 1961.

ADHESION OF SPHERICAL PARTICLES TO PLANE SURFACES

by

N.L. Cross and H. Stretch

INTRODUCTION

A knowledge of the basic mechanism underlying the retention of fall-out particles on surfaces is helpful in developing effective decontamination techniques. In particular it is important to find out whether radioactive and inactive particles behave similarly in their adhesion to surfaces under various conditions of humidity, so that a correct interpretation may be placed on results of field trials obtained with inactive simulants.

Information of this kind is not to be found in published literature, so a study as described in the title was undertaken. In it, glass, quartz, and platinum inactive spheres and plane surfaces, and radioactive glass spheres, were examined in both water and alcohol vapour/air atmospheres. A direct weighing procedure based on the use of a modified quartz fibre torsion balance was used, making it possible to measure the adhesion force with considerable accuracy, first balancing out the particle mass; a feature not previously described in adhesion measurement techniques.

APPARATUS

The apparatus consisted essentially of a torsion balance and a humidity chamber. The chamber was positioned below the balance so that particles under examination could be suspended from a balance stirrup into the working area of the chamber.

Torsion Balance

A torsion balance was constructed, based on a design by El-Badry and Wilson (1), from quartz fibres. Each part of the balance, e.g. beam, quartz bow, torsion fibre, etc., was made by supporting selected fibres, suitably placed in position on glass microscope slides and glueing them at overlapping points with Durofix diluted 1:4 with amyl acetate. When the joints were dry, all superfluous fibre was removed with a sharp knife.

RESTRICTED

Finally, the beam was cemented centrally across the torsion fibre - quartz bow, and fine fibres, to which weight stirrups were fastened, suspended from each end. The completed unit was mounted in a Perspex case; one end of the torsion fibre was retained in a slow motion dial on the front of the case, the other in a terminal at the back. This terminal was capable of rotation, in order to set the zero reading on the dial, and of reciprocation, so that tension in the fibre could be adjusted. By fitting the dial with a vernier, $1/2000$ th of a complete revolution could be measured. Weights could be placed on the stirrups, or the different particles under test suspended in the humidity chamber, by lifting up the sides of the balance case.

The dimensions of the fibres used in constructing the beam and torsion fibre assembly are shown in Fig. 1, and Fig. 12 is a photograph of the balance.

Certain modifications were made to the design of El-Badry and Wilson, as follows:

1. An optical method for the determination of point of balance was not used. Instead, an index fibre, projecting from the end of the beam, was allowed to move between two scales, the front one of Perspex, the rear engraved on brass, and the balance point determined by a parallax procedure.
2. When the adhesive force was greater than the opposing force which could be supplied by the torsion fibre alone, the latter was implemented by adding weights in the form of stainless steel riders.
3. To avoid separating the adhering surfaces by impact, on adding the riders, adjustable stainless steel knife edges were arranged to arrest the beam.

A calibration curve, obtained by plotting dial readings against known weights (the riders) is shown in Fig. 2.

Humidity Chamber

Essentially this consisted of two Perspex boxes, one inside the other, mounted on a common base. A few holes were drilled in the inner box to permit the free circulation of air.

A square Perspex chimney was positioned centrally through both boxes, terminating at the base of the balance. The fibre supporting the test particle was hooked to a weight stirrup, then passed through the balance case base, as described under 'Technique of Measurement', into the chimney, terminating directly above a platform on which the test plane surface was placed. This platform was capable of being raised or lowered by means of a screw passing through the base of the humidity chamber. In addition since it was frequently necessary to clean the test surfaces, the complete platform unit could rapidly be removed from the chamber.

RESTRICTED

U. S. ~~RESTRICTED~~ CONFIDENTIAL
MODIFIED HANDLING AUTHORIZED

In the first experiments, stray electrostatic effects were dissipated by placing radioactive materials in close proximity to the test surfaces, and also by lining the inner box with copper foil, suitably earthed through a low resistance path. Later, active materials were found unnecessary and omitted. Finally observation ports through the lining were provided.

A photograph of the chamber and a diagram illustrating the details of the chimney and platform assembly are appended as Fig. 13 and Fig. 3 respectively. Fig. 14 shows the complete assembly.

Humidity

Known humidities were obtained inside the chamber by introducing concentrated salt solutions of known saturation vapour pressure (for details see ref. 2). The appropriate solutions were contained in 30 ml beakers situated in the corners of the chamber away from the humidity measuring element, and in order to hasten the attainment of equilibrium, rolls of filter paper about 6 in. long were placed in the beakers and a small fan used to stir the humid air.

The 'Gregory' electrolytic hygrometer was finally selected to be the monitoring element. The advantages and disadvantages which are found with this type of hygrometer are outlined by Ponman (3). The element was placed in a corner of the outer humidity box and excited with a.c. through a high value resistor from a suitably loaded constant voltage transformer. The potential drop across the element, corresponding to a particular humidity, was indicated on an a.c. valve voltmeter. Temperature was recorded by means of a thermometer placed as near as possible to the contacting surfaces.

A calibration curve was prepared as follows:

The element, previously fixed into a rubber bung, was inserted into a 32 oz. bottle, immersed in a thermostat at 24.5°C, containing a saturated salt solution of known saturation vapour pressure and voltages recorded until a constant reading, corresponding to equilibrium humidity condition above the liquid, was reached. A plot of voltage against humidity (recorded as relative humidity at 24.5°C) for a number of different solutions was prepared, Fig. 4, and used in conjunction with a set of temperature compensation curves supplied by the manufacturers of the element, in order to ascertain the humidity conditions existing inside the chamber during adhesion measurement.

Further modifications and additions to the apparatus were required in order that adhesion measurements could be made below 18% R.H. Initial attempts to attain these lower humidities were unsuccessful because too much water vapour diffused into the balance and humidity chamber from the surrounding air. Consequently the whole apparatus was mounted inside a large glove box: Fig. 5. At the lower humidities large static charge effects reappeared, and were eliminated by lining the whole of the balance box and chimney with stiff copper gauze and earthing it. Entry to the balance was made through a hinged flap in one side of the gauze cube, the mesh of the gauze being such that the balance could be easily seen.

U. S. ~~RESTRICTED~~ CONFIDENTIAL
MODIFIED HANDLING AUTHORIZED

RESTRICTED

TECHNIQUE OF MEASUREMENT

1. Preparation of the bead suspension unit.

A bead of the required size was fashioned on the end of a fibre prepared from the test material and excess fibre cut off so that a stem 0.5-1 cm remained. A cellulose acetate fibre, 5-15 μ diameter, was fastened to the stem with diluted Durofix, and the other end cemented to a small hook made from fine copper wire.

2. Procedure for cleaning the bead and test plane surface.

Beads were cleaned by immersion in isopropyl alcohol vapour for 5 minutes according to the method described by Putner (4). It was not very practical to clean plane surfaces in this way; instead they were treated with Teepol solution, washed with water, placed in position on the measurement platform, then dried as quickly as possible with grease-free filter paper and allowed to attain equilibrium in the humidity chamber.

3. Operation of the balance.

Prepared bead units were lowered through the balance case into the humidity chamber, after attachment to the weight stirrup. Suitable riders were placed on the balance and the beam freed by lowering the knife edges. Balance point was found by rotating the torsion fibre, and the rider weights and dial reading recorded. Next the platform was raised until contact was made between bead and plane surface, and torsion applied to the fibre, weights added, etc. as quickly as possible, until a separation was achieved. The new weights and dial readings were recorded, and the adhesion force found from the difference between readings.

4. Bead size determination

After selecting the bead samples for symmetry, surface smoothness and size range, diameters were measured at right angles to the stem, using a travelling microscope.

RESTRICTED

RESTRICTED

ADHESION OF INACTIVE PARTICLES

Experimental

The following results were obtained:

1. Adhesion in saturated atmospheres

TABLE 1.

(water vapour atmosphere)

Bead radius μ	Glass on glass Adhesion (dynes)	% theory* (Z=4.17y)
117.5	9.91	92
171	13.21	84
174	13.39	84
220	16.50	82
290	21.95	83
421	33.05	85

TABLE 2.

(water vapour atmosphere)

Bead radius μ	Glass on quartz Adhesion (dynes)	% theory
117.5	9.5	88
220	16.45	82
290	21.9	83
421	32.35	84

* The theory developed in the appendix of this report is unsuitable for routine calculation of adhesion force, since it necessitates the very precise measurement of relative humidity.

RESTRICTED

RESTRICTED

TABLE 3.

(water vapour atmosphere)

Bead radius μ	Platinum on platinum Adhesion (dynes)	% theory
464	12.12	29
511	12.91	28

TABLE 4.

(n-propanol vapour atmosphere)

Bead radius μ	Glass on glass Adhesion (dynes)	% theory
117.5	3.53	100
220	5.4	82
290	7.46	86
421	9.95	79

2. Adhesion in 45-52% R.H. water vapour atmospheres

TABLE 5.

Bead radius μ	% R.H.	Glass on glass Adhesion (dynes)
218	49	0.052
225	52	0.101
294	47	0.258
350	45	0.05
361	48	0.043
379	48	0.145
442	47	0.124
532	50	0.173
575	52	0.049
591	48	0.046

RESTRICTED

RESTRICTED

3. Adhesion in 16-18°/o R.H. water vapour atmospheres

TABLE 6.

Bead radius μ	°/o R.H.	Glass on glass Adhesion (dynes)
222	18	0.075
387	17	0.132
538	16	0.195

4. A wide range of values could be obtained for all beads in 66-88°/o R.H. atmospheres, suggesting that in this region large changes in adhesion resulted from relatively small humidity changes.

5. Adhesion of a bead fully immersed in water

TABLE 7.

Bead radius μ	Adhesion (dynes)	°/o theory (see Appendix)
750	33.6	103

DISCUSSION

McFarlane and Tabor (5) showed that adhesion/humidity curves derived from experimental data obtained using glass surfaces were similar to curves prepared by McHaffie and Lenher (6), in which °/o R.H. was plotted against calculated values of film thickness of water deposited on glass surfaces at the appropriate humidity (the weight of water per unit area was found experimentally). The curves showed no measurable adhesion below about 75°/o R.H. then rose steeply to denote strong adhesion at 85°/o R.H., and maintained this value to saturation.

In addition they demonstrated that in high humidity atmospheres adhesion resulted essentially from the surface tension of a liquid film formed between the surfaces in contact, in accordance with the expression

$$Z = 4\pi R\gamma \cos \alpha$$

in which Z is the adhesion force in dynes, γ the surface tension of the liquid in dynes per cm, α the contact angle, and R the sphere radius. None of the experimental results agreed too well with the predicted figures, all results being 10-20 per cent on the low side.

RESTRICTED

RESTRICTED

The results obtained in the present study compare with those of McFarlane and Tabor as follows:-

- i. Similar results are obtained with both glass and quartz surfaces at high humidity values, once again figures being 10-20 per cent below those predicted.
- ii. As a consequence of the greater sensitivity of measurement attainable with the torsion fibre balance, adhesion at lower humidities has been measured.
- iii. Similar low results are obtained with platinum surfaces, due to incomplete wetting (an alternative explanation was offered by McFarlane and Tabor).
- iv. Whereas previously adhesion has not been shown in alcohol saturated atmospheres, in the present study values within 10-20 per cent of the predicted amount have been measured.

Reference to the thesis by McFarlane, on which the paper by McFarlane and Tabor (5) was based, indicated that certain assumptions used to derive the expression given previously were in error. One such was that the liquid meniscus thickness was always small, but in fact, experimental work demonstrated that thickness increased markedly as saturation humidity was approached, so that while the effect might be of little significance with large beads, it must be considered when the bead radius was less than 1 mm. In consequence a revised expression was calculated, as shown in the appendix, which includes Figs. 6 (a-d) to illustrate the argument.

Theoretical variation of meniscus thickness with relative humidity, for two bead sizes, is shown in Fig. 7, and the relation between the associated variable θ (the semi-angle subtended at the bead centre by the meniscus), and bead radius and humidity, is illustrated in Fig. 8 as derived from the expression

$$\ln \frac{p}{p_0} = \frac{2\gamma M}{R\rho RT} \left\{ \frac{\cos \theta}{1 - \cos \theta} \right\} - \text{see appendix}$$

The decrease in adhesion as saturation humidity is approached is shown as Fig. 9.

Finally, although the values recorded in Tables 1-4 are 8-18% below those predicted by McFarlane and Tabor, they accord with revised theory when the relative humidity at the time of measurement is very close to saturation.

RESTRICTED

RESTRICTED

ADHESION OF RADIOACTIVE PARTICLES

1. Preparation of radioactive heads

Suitable glass fibres were taken and a bead fashioned in the blow-pipe flame. The hot bead was brought into contact with a minute quantity of europium oxide, and the whole fused until the oxide appeared to be distributed uniformly throughout. Fusion was continued until the bead appeared to be spherical and free from prominences when examined under a microscope.

The beads were sized with a travelling microscope and submitted for neutron irradiation.

The following table shows the bead sizes and the activity measured on the second shelf of a castle containing an end-window Geiger tube. Overall counting efficiency was about 3 %.

TABLE 8.

Bead radius	c.p.m.	c.p.m./radius (cm)
284 μ	13,300	4.7×10^5
320 μ	5,400	1.7×10^5
450 μ	5,000	1.1×10^5
503 μ	6,400	1.3×10^5
519 μ	11,000	3.8×10^5

Before counting, Na^{24} was allowed to decay.

Europium is found as a mixture of two isotopes, Eu^{151} in 48.8% abundance and Eu^{153} as the remainder. Eu^{152} has two modes of decay, one of 13 year half-life with emission of a 0.7 Mev beta radiation (the excitation cross-section for this form is 3,360 barns), the other of 9.2 hour half-life with emission of a 1.8 Mev electron (cross-section for this form 670 barns). Eu^{154} has a 16 year half-life and an excitation cross section of 125 barns. It may be concluded that the bulk of the activity associated with the beads resulted from 13 year Eu^{152} .

RESTRICTED

RESTRICTED

EXPERIMENTAL

The following results were obtained.

TABLE 9.

Bead radius μ	% R.H.	Glass to glass Adhesion (dynes)
320	18	4.55
450	18	3.17
519	18	2.89
387	47	2.95
284	48	4.33
320	48	3.98
392	48	2.82
450	48	2.30
392	51	1.18
392	53	0.83
392	54	0.83
346	56	0.87
284	58	1.36
387	61	0.79
450	61	0.45
500	61	0.40
450	saturated	20.0 This was the highest value in a series.

The results are shown graphically in Fig. 10, and expressed as an equation

$$Z = ke^{-sR}$$

in which Z is the adhesion force in dynes, k is the force when the charge producing the adhesion is concentrated at the point of contact, and depends on the dielectric properties of the bead (k is shown on the graph as the adhesion force for a sphere of zero radius), s a parameter concerned with charge loss, and R the sphere radius.

Values of s obtained by substitution in the above expression at different humidities were plotted against % R.H. to yield a curve sensibly flat at low humidities but rising steeply at about 50% R.H. The minimum reading appeared to be concerned with loss of charge in dry air. The curve beyond 50% R.H. was similar to those prepared by Curtis (7) from measurements of D. C. leakages over Pyrex surfaces at various humidities, so that charge loss resulted from increased conductance over the surfaces in contact.

RESTRICTED

RESTRICTED

It would seem that when adhesion results essentially from electrostatic charge built up on a dielectric surface as a consequence of the decay of incorporated radioactive matter, the sorption of water vapour on the contacting surfaces causes weaker adhesion. At a certain humidity, however, this loss is cancelled by increasing adhesion resulting from surface tension, so that a further rise in humidity produces marked adhesion once again.

An equivalent circuit may be used to represent the charging conditions in dry air. Active material is represented as a generator A producing a current i , and the spherical particle by a capacitor C . R is the total resistance resulting from the particle and air resistances.

The voltage developed will be $v = Ri (1 - e^{-t/RC})$,
 t being measured from the time at which charging commenced.

Attempts to evolve a more logical quantitative explanation of the adhesion effect due to incorporated radioactivity were unsuccessful because of the difficulty in establishing any charge-activity relation. Experimentally, a surface potential measurement procedure was examined first, and when this failed to yield any conclusive information, it was replaced by an attempt to measure charge on a bead, using a modification of Millikan's method. This involved suspending the bead between charged plates and comparing the deflection with that shown by a similar inactive specimen. Both methods failed because of the difficulty of eliminating charges, of much the same intensity as the radioactive charge, which were produced in other ways. Unfortunately, any ideas of increasing the wanted effect by increasing the activity are likely to be offset by difficulties in handling the bead.

CONCLUSION

The investigation shows that a significant increase in adhesion may occur in radioactive spherical dielectric particles, as compared with similar inactive particles, in low relative humidity conditions. At higher humidities, where adhesion results from surface tension forces, no difference can be detected between active and inactive particles.

ACKNOWLEDGEMENT

Dr. R.G. Picknett assisted with the theoretical evaluation of inactive particle adhesion.

(Sgd.) H.L. Green,
Supt., Physics Research Division.

NLC/HS/RT

(Sgd.) A.S.G. Hill,
Deputy Director.

RESTRICTED

RESTRICTED

1. H.M. El-Badry and O.L. Wilson Report of a symposium on
microbalances, p. 36, Sept. 1959.
Royal Institute of Chemistry.
2. International Critical Tables 1, p. 68
3. H.L. Penman Humidity, p. 55 1955. Institute of
Physics.
4. T. Putner Brit. J. Appl. Phys. 10 (7), 332-6,
1959.
5. J.S. McFarlane and D. Tabor Proc. Roy. Soc., A202, p. 224, 1950.
6. I. R. McHaffie and S. Lenher J. Chem. Soc., 127, p. 1559, 1925.
7. H.L. Curtis U.S. Bureau of Standards, Scientific
Paper No. 234.

RESTRICTED

RESTRICTED

APPENDIX TO P.T.P. (R)- 35

The liquid film between a bead and plate

To evaluate the adhesion force caused by the film it is necessary to determine the principal radii of curvature at all points on the liquid surface. By definition, the centres of curvature for a given point on a surface must lie normal at that point. Also by definition, the principal curvatures lie in planes such that the curvatures are maximum and minimum.

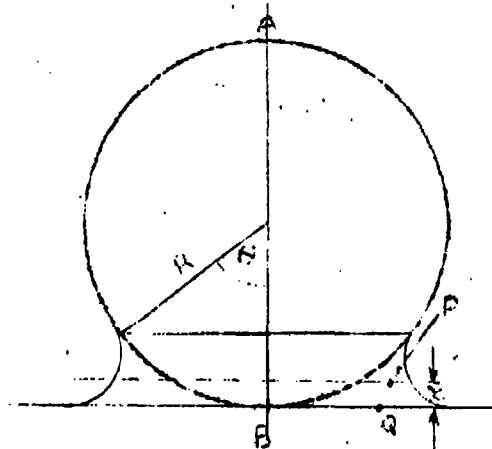
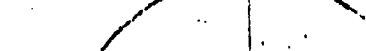


FIG. 6a.

The effect of hydrostatic pressure

The pressure at P is related to the pressure at Q by the relation;

$$p_p = p_q - \rho g x \quad \text{where } g = \text{acceleration (gravity)}$$

$$\rho = \text{density liquid}$$

Using this equation, the force towards the centre of the sphere exerted by the pressure in the film is:

$$\int_0^\theta \left\{ p_q - g_p R (1 - \cos \alpha) \right\} 2\pi R^2 \sin \alpha d\alpha, \text{ where } \alpha \text{ is the contact angle.}$$

RESTRICTED

RESTRICTED

The vertical force on the sphere is:

$$\int_0^\theta \left\{ p_q - g_p R (1 - \cos \alpha) \right\} 2\pi R^2 \sin \alpha \cos \alpha d\alpha$$

$$\text{i.e. } p_q \pi R^2 \sin^2 \theta + \pi R^3 g_p \left\{ \frac{2}{3} (1 - \cos^3 \theta) - \sin^2 \theta \right\}.$$

Atmospheric pressure P_1 acting on the sphere gives an opposing force of $\pi R^2 P_1 \sin^2 \theta$.

The net force on the sphere due to pressure is therefore

$$(P_1 - p_q) \pi R^2 \sin^2 \theta - \pi R^3 g_p \left\{ \frac{2}{3} (1 - \cos^3 \theta) - \sin^2 \theta \right\}$$

As will be shown later, $(P_1 - p_q)$ is never smaller than $0.35 \gamma/R$ i.e. for $\gamma = 70$ dyne/cm, $(P_1 - p_q) > \frac{24}{R}$ dyne/cm². Thus, when R is of the order 100μ radius, the second term of the above expression for the force is negligible compared to the first term ($< 1\%$).

Therefore the effect of hydrostatic pressure can be neglected in all pressure and force calculations when R is of the order 100μ or smaller.

Since the hydrostatic pressure is negligible, the pressure inside the film is constant at all points, and the pressure difference ΔP across the surface is also constant,

$$\text{i.e. } \gamma \left\{ \frac{1}{r_1} + \frac{1}{r_2} \right\} = \Delta P, \text{ where}$$

r_1 and r_2 are the principal radii of curvature for a point on the liquid surface.

RESTRICTED

Determination of the pressure difference across the liquid surface(a) Zero contact angles

In Fig. 6b, the curve HIJ representing the surface of the liquid film is defined by the equation

$$\frac{1}{r_1} + \frac{1}{r_2} = \text{constant}$$

where r_1 and r_2 are the principal radii of curvature for any point P on the surface. The sign convention adopted is that the radius of curvature is positive if it does not pass through the liquid of the film.

$$\text{Thus } \frac{1}{PL} - \frac{1}{PK} = \text{constant.}$$

When P is at H, the point of contact of the liquid with the sphere, then $r_2 = R$. As P moves towards I, r_2 decreases and is a minimum when P equals I. I is where the tangent to the curve is parallel with OK. r_1 also is at a minimum at this point. As P moves from I to J, r_2 and r_1 increase again and at J $r_2 = \infty$ and $r_1 = \text{constant}$. Thus the curve HIJ is by no means circular. The curvature constantly changes as

does the centre of curvature. Mathematically, it proved too complicated to solve analytically the differential equation $\frac{1}{r_1} - \frac{1}{r_2} = \text{const}$ to give r_1 and r_2 in terms of R and θ , therefore a graphical method was used.

For simplicity, the angles of contact were assumed to be zero. With a given R and θ , a likely value of r_1 was chosen for point H and the constant in the equation evaluated using $R = (r_2)_H$, (i.e. $r_2 = R$ at point H).

Starting from H, the curve HIJ was constructed in small steps: at each step r_2 being measured and r_1 calculated together with the new centre of curvature. When point J was reached, inspection showed whether the initial assumed value of r_1 at H was too large or too small for the curve just to touch the line ST representing the plate surface. Thus by successive approximation the correct value of $(r_1)_H$ was obtained. AP then followed from the equation:

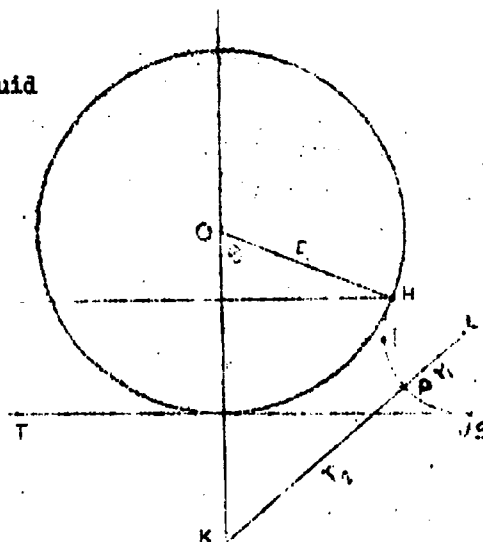


FIG. 6b

$$\Delta P = \gamma \left\{ \frac{1}{(r_1)_H} - \frac{1}{R} \right\}$$

$(r_1)_H$ is the value of r_1 at H.

The process was repeated for various values of θ and it was found that $(r_1)_H$ closely approximated to the radius of the osculatory circle which touches the sphere at H and the plate at J.

$$\text{i.e. } (r_1)_H = \frac{R(1 - \cos\theta)}{(1 + \cos\theta)}$$

For the range $0 < \theta < 65^\circ$ the difference between this radius and $(r_1)_H$ was always less than about 6% of $(r_1)_H$. For $\theta < 5^\circ$ no difference could be detected.

The error curve is shown as Fig. 11.

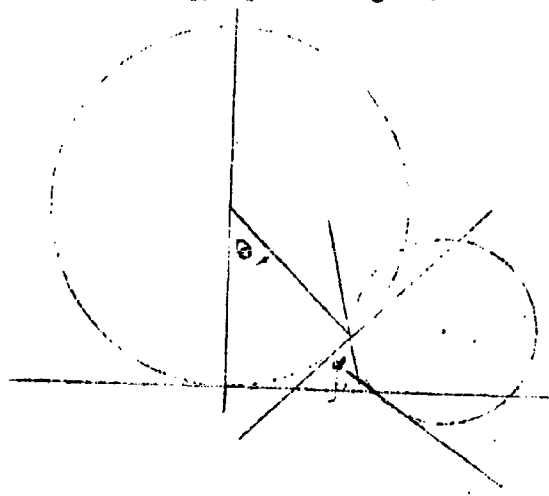
The conclusion is that the following gives ΔP to within 6% error in the range shown:

$$\Delta P = \frac{2\gamma}{R} \left\{ \frac{\cos\theta}{1 - \cos\theta} \right\} \quad 0 < \theta < 65^\circ$$

(b) finite contact angles

This approach can presumably be extended to the case where the angles of contact α or β are finite, by using the radius of the circle which cuts the sphere and the plate at the appropriate angles.

FIG. 8c



RESTRICTED

In Fig. 6c the radius of circle = $\frac{R(1 - \cos\theta)}{\cos\beta + \cos(\theta + \alpha)}$

$$= (r_1)_H \text{ (assumed)}$$

$$\text{whence } \Delta P = \frac{\gamma}{R} \left[\frac{\cos\theta + \cos\beta + \cos(\theta + \alpha) - 1}{1 - \cos\theta} \right]$$

No measurement has been made of the accuracy of the approximation in this case, but comparison indicates that the larger α and β , the smaller the range of θ for which the approximation is reasonably accurate.

Force on bead in contact with the plate

Zero contact angle assumed for simplicity. Force on bead due to the liquid film:

$$Z = 2\pi R \gamma \sin^2 \theta + \pi R^2 \Delta P \sin^2 \theta$$

$$\text{using } \Delta P = \frac{2\gamma}{R} \left\{ \frac{\cos\theta}{1 - \cos\theta} \right\}$$

$$Z = 2\pi R \gamma (1 + \cos\theta)$$

As $\theta \rightarrow 0$, $Z \rightarrow 4\pi R \gamma$

This is accurate because the error in the approximation for $(r_1)_H$ is zero for very small θ .

$$\text{As } \theta \rightarrow \frac{\pi}{2}, Z \rightarrow 2\pi R \gamma$$

Due to the approximation for $(r_1)_H$ this is some 15% low. The correct value for Z is 2.35 $\pi R \gamma$ (from the graphical solution).

Force to remove bead from plate

If, as the bead is lifted from the plate, the force on it increases before finally decreasing, then the force to remove the bead will not equal the force on the bead when in contact with the plate. If, on the other hand the force decreases as the bead is lifted, then the force required to remove the bead will equal the force when in contact with the plate.

To decide between the two, necessitates the calculation of the volume of the liquid film and $(r_1)_H$ and θ for various distances of separation between the bead and plate. The general calculation is very complicated and has not been carried out.

RESTRICTED

RESTRICTED

A simple approximation has been used which is accurate for small θ and small h taking the liquid as a cylinder as shown.

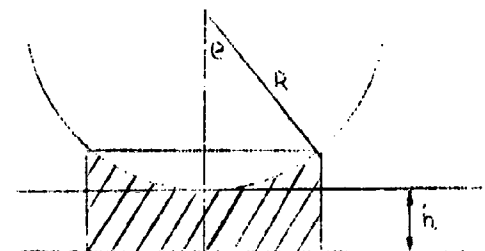


FIG. 6d

In Fig. 6d the volume of liquid, V , is given by

$$V = \pi R^3 \sin^2 \theta \left\{ \frac{h}{R} + 1 - \cos \theta \right\} - \frac{\pi R^3}{3} (1 - \cos \theta)^2 (2 - \cos \theta)$$

Radius of osculatory circle r :

$$\frac{r}{R} = \frac{\frac{h}{R} + (1 - \cos \theta)}{(1 + \cos \theta)}$$

V remains constant. $\frac{V}{\pi R^3}$ is determined for a given value of θ .

$h = 0$. $\frac{r}{R}$ is also determined.

Then θ is reduced slightly and $\frac{h}{R}$ calculated. Using this value $\frac{r}{R}$ is recalculated.

Typical example

$$\theta = 5^\circ, h = 0, \frac{V}{\pi R^3} = 2.75 \times 10^{-5}, \frac{r}{R} = 1.90 \times 10^{-3}$$

$$\theta = 4.5^\circ, \frac{h}{R} = 1.82 \times 10^{-3}, \frac{V}{\pi R^3} \text{ as before } \frac{r}{R} = 2.46 \times 10^{-3}$$

This shows that as h increases, θ decreases and r increases

$$\text{As } \Delta P = \frac{\gamma}{R} \left\{ \frac{2 \cos \theta - \frac{h}{R}}{\frac{h}{R} + 1 - \cos \theta} \right\}, \Delta P \text{ must decrease as } h \text{ increases,}$$

RESTRICTED

RESTRICTED

therefore Z must decrease as h increases.

The indication is that the force on the bead is at a maximum when the bead is in contact with the plate.

Hence, tentatively, the force to remove the bead from the plate is

$$Z = 2\pi RY (1 + \cos\theta)$$

TABLE 1.

Generalised values of ΔP

θ°	ΔP using radius of osculatory circle	ΔP using result obtained graphically	% Error in using osculatory radius for ΔP
5	523 $\frac{Y}{R}$	523 $\frac{Y}{R}$	0
13	75.3 $\frac{Y}{R}$	74.3 $\frac{Y}{R}$	2
26	17.7 $\frac{Y}{R}$	16.8 $\frac{Y}{R}$	5
30	13.0 $\frac{Y}{R}$	12.2 $\frac{Y}{R}$	6
45	4.81 $\frac{Y}{R}$	4.55 $\frac{Y}{R}$	6
60	2.00 $\frac{Y}{R}$	1.97 $\frac{Y}{R}$	2
75	0.71 $\frac{Y}{R}$	0.85 $\frac{Y}{R}$	-16
90	0.00 $\frac{Y}{R}$	0.35 $\frac{Y}{R}$	$-\infty$

RESTRICTED

RESTRICTED

TABLE 2.

Generalised values of Z

θ	$\frac{Z}{R\gamma}$ using radius of osculatory circle	$\frac{Z}{R\gamma}$ using result obtained graphically
0	12.57	12.57
5	12.55	12.55
13	12.40	12.13
26	11.92	11.34
30	11.73	11.17
45	10.72	10.30
60	9.43	9.36
75	7.91	8.35
90	6.28	7.38

Film in Equilibrium with air at fixed vapour pressure

The Gibbs-Kelvin equation may be expressed in the form:

$$\ln \frac{p}{p_0} = - \frac{\gamma M}{p R T} \left\{ \frac{1}{r_1} + \frac{1}{r_2} \right\}, \text{ where}$$

p = vapour pressure over film
 p_0 = vapour pressure plane liquid surface
 M = mol. wt. liquid in vapour
 ρ = density liquid
 R = gas constant
 T = temperature (absolute)

It has been shown previously that

$$\left\{ \frac{1}{r_1} + \frac{1}{r_2} \right\} = \left\{ \frac{(1 + \cos \theta)}{R(1 - \cos \theta)} - \frac{1}{R} \right\} = \frac{2 \cos \theta}{R(1 - \cos \theta)}$$

$$\text{Hence } \ln \frac{p}{p_0} = - \frac{2 \gamma M}{R \rho R T} \left\{ \frac{\cos \theta}{1 - \cos \theta} \right\}$$

Thus for a given value of the relative humidity of the air, there is one value of θ for which the film is in equilibrium.

RESTRICTED

RESTRICTED

SUMMARY

1. Hydrostatic pressure may be neglected with small beads.
2. The pressure inside the film is constant at all points.

$$\Delta P = \gamma \left(\frac{1}{r_1} + \frac{1}{r_2} \right) = \text{constant}$$

$$3. \quad \Delta P = \frac{2\gamma}{R} \left\{ \frac{\cos\theta}{1 - \cos\theta} \right\} \quad \begin{array}{l} 0 < \theta < 65^\circ \\ \text{error} < 6\% \end{array}$$

zero contact angles

4. Correct values of ΔP , $0 < \theta < 90^\circ$ are shown in a table.
5. For finite contact angles α or β :

$$\Delta P \approx \frac{\gamma}{R} \left\{ \frac{\cos\theta + \cos\beta + \cos(\theta + \alpha) - 1}{1 - \cos\theta} \right\}$$

6. Force on bend due to film

$$Z = 2 \pi R \gamma (1 + \cos\theta).$$

7. It may be tentatively assumed that this is the force required to remove the bead.

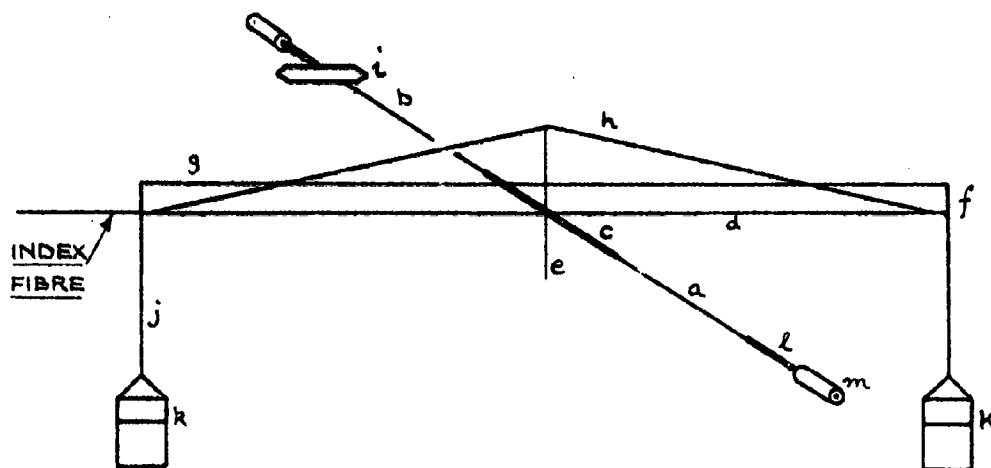
8. The equilibrium value of θ for air of fixed vapour pressure is given by:

$$\ln\left(\frac{p}{p_0}\right) = \frac{-2\gamma M}{\rho R T} \left\{ \frac{\cos\theta}{1 - \cos\theta} \right\}$$

zero contact angles

RESTRICTED

BEAM & TORSION FIBRE ASSEMBLY.



DIMENSIONS OF FIBRES USED.

	<u>LENGTH (cm)</u>	<u>DIAM (APPROX)</u> <u>(MICRONS)</u>
(a) <u>FRONT TORSION FIBRE.</u>	5	20-40
(b) <u>REAR TORSION FIBRE.</u>	5	20-40
(c) <u>CROSS HORIZONTAL MEMBER.</u>	2	150
(d) <u>MAIN HORIZONTAL MEMBER.</u>	10+1 (INDEX)	240
(e) <u>MAIN VERTICAL MEMBER.</u>	1 ABOVE 'd', 1 BELOW.	145
(f) <u>SIDE VERTICAL MEMBERS.</u>	0.2 - 0.3	100
(g) <u>HORIZONTAL BRACE FIBRE.</u>	10	40
(h) <u>BRACE FIBRES.</u>	5.1	80
(i) <u>QUARTZ BOW</u>	2.6 X 0.3	120
(j) <u>SUSPENSION FIBRES (CELLULOSE</u> <u>ACETATE.)</u>	5	5-10
(k) <u>STIRRUPS.</u>	2.3 X 0.6	80
(l) <u>QUARTZ STEMS.</u>		250
(m) <u>CAPILLARY NIPPLES.</u>	<u>1/4" DIAM X 1/4" LONG.</u>	<u>350 BORE.</u>

FIG. 1

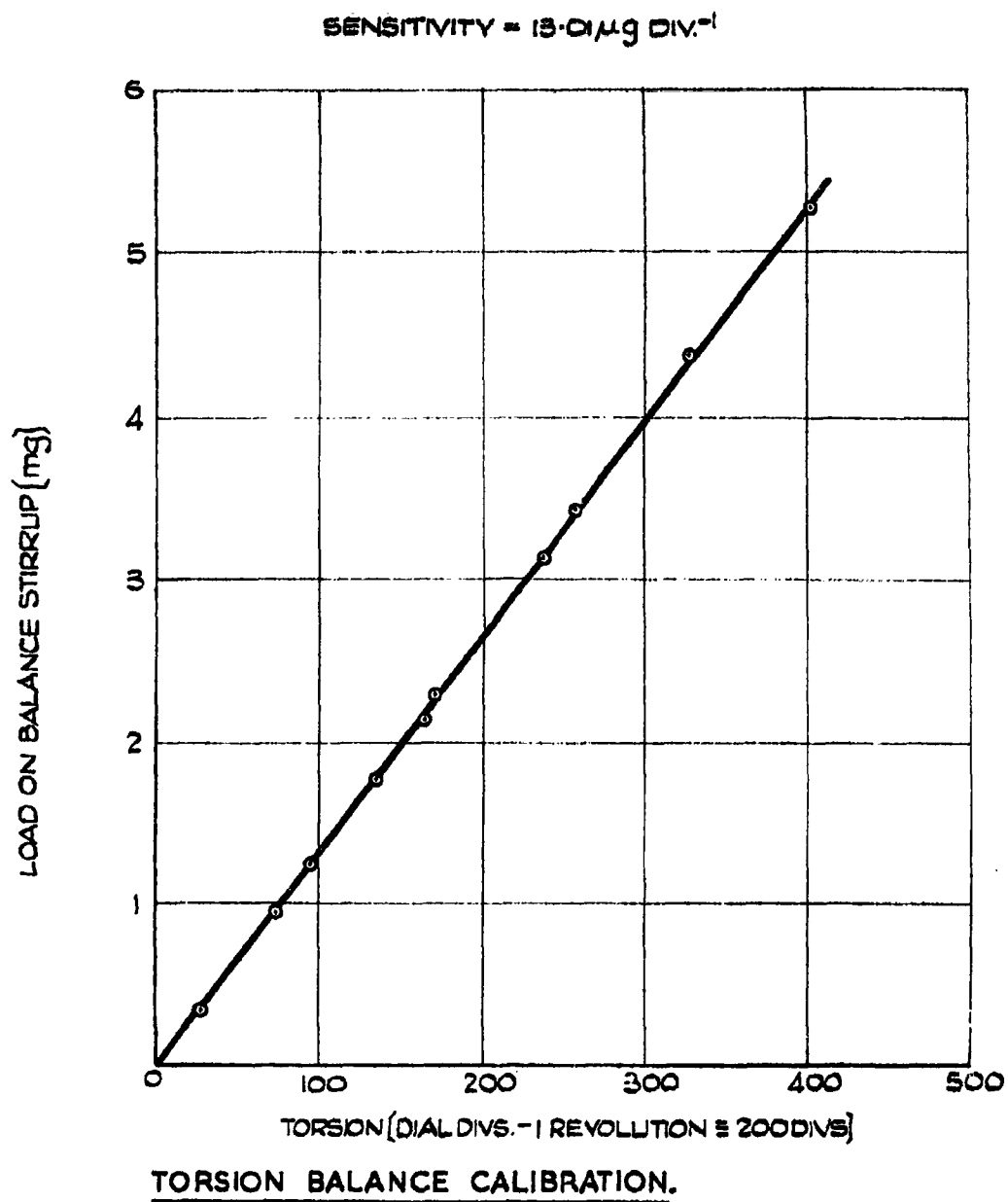


FIG. 2.

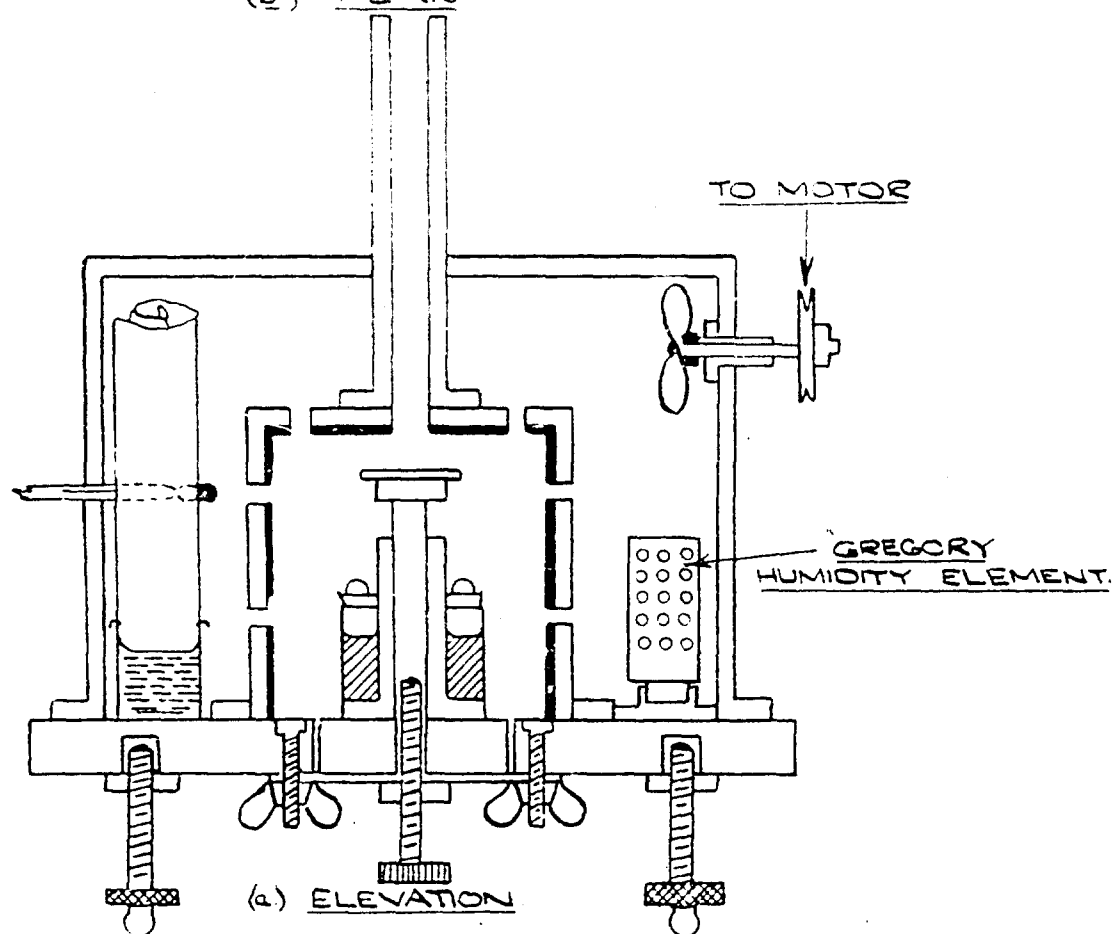
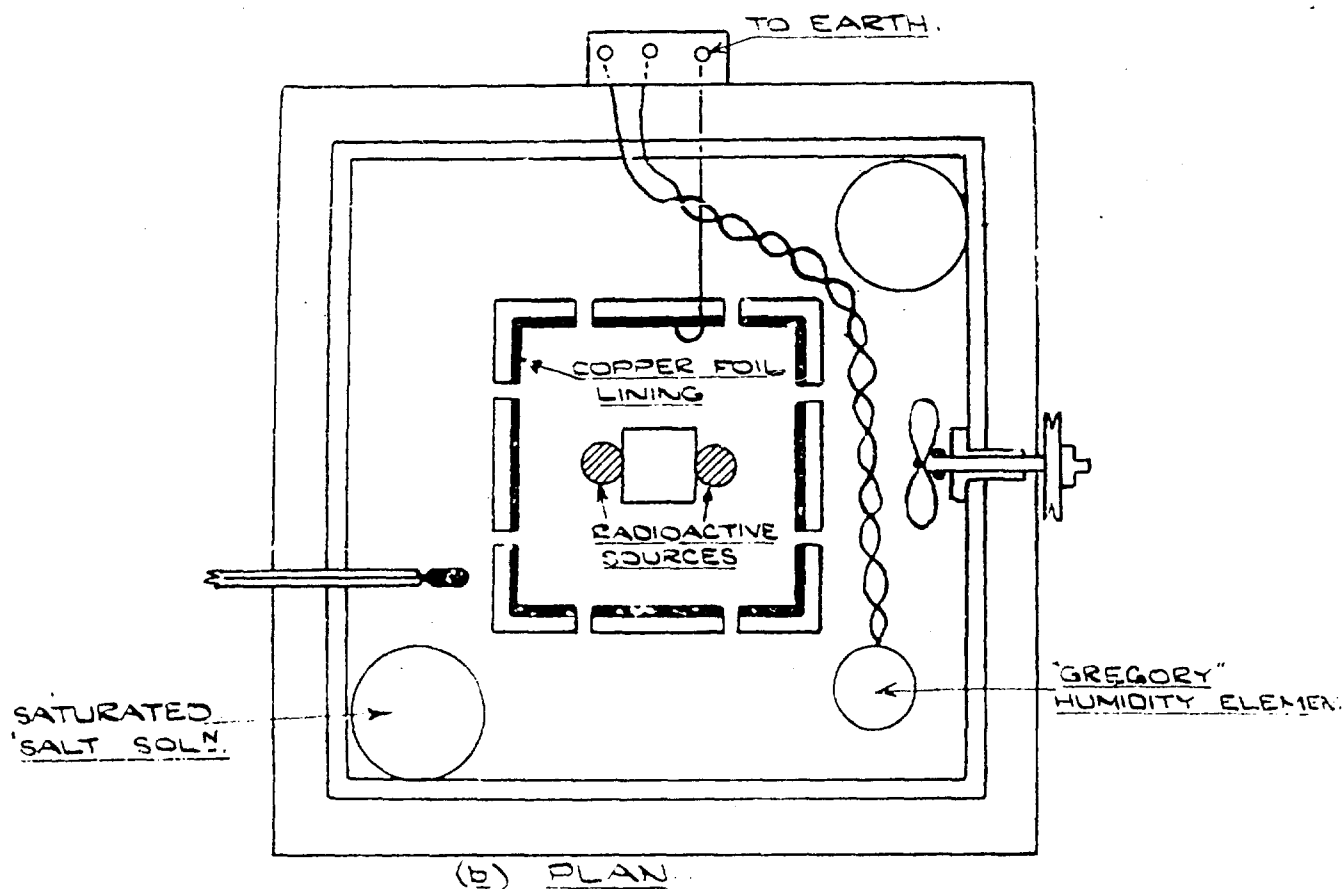


FIG. 3

THE HUMIDITY CHAMBER.

(SCALE: 1 CM = 1 INCH.)

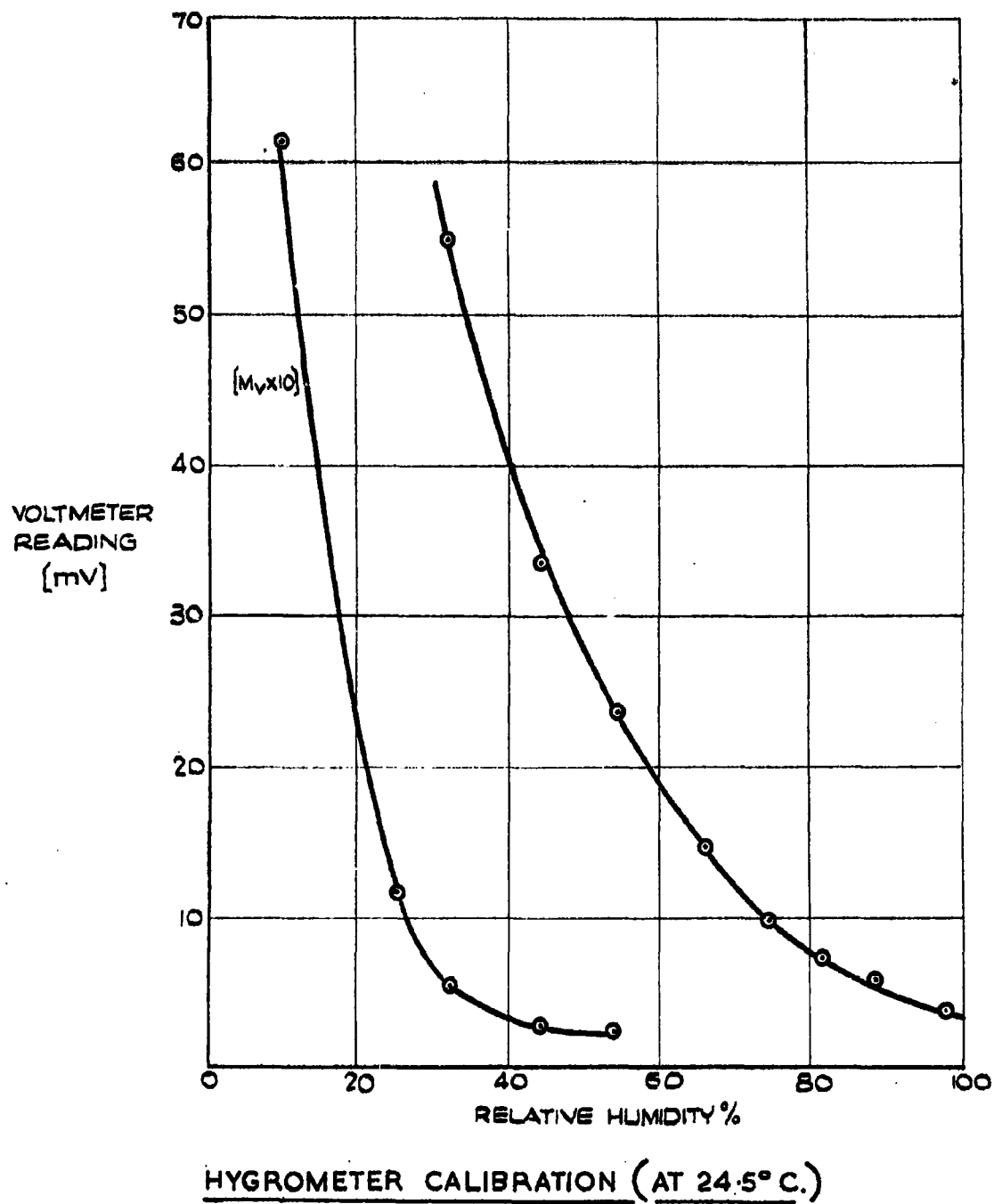
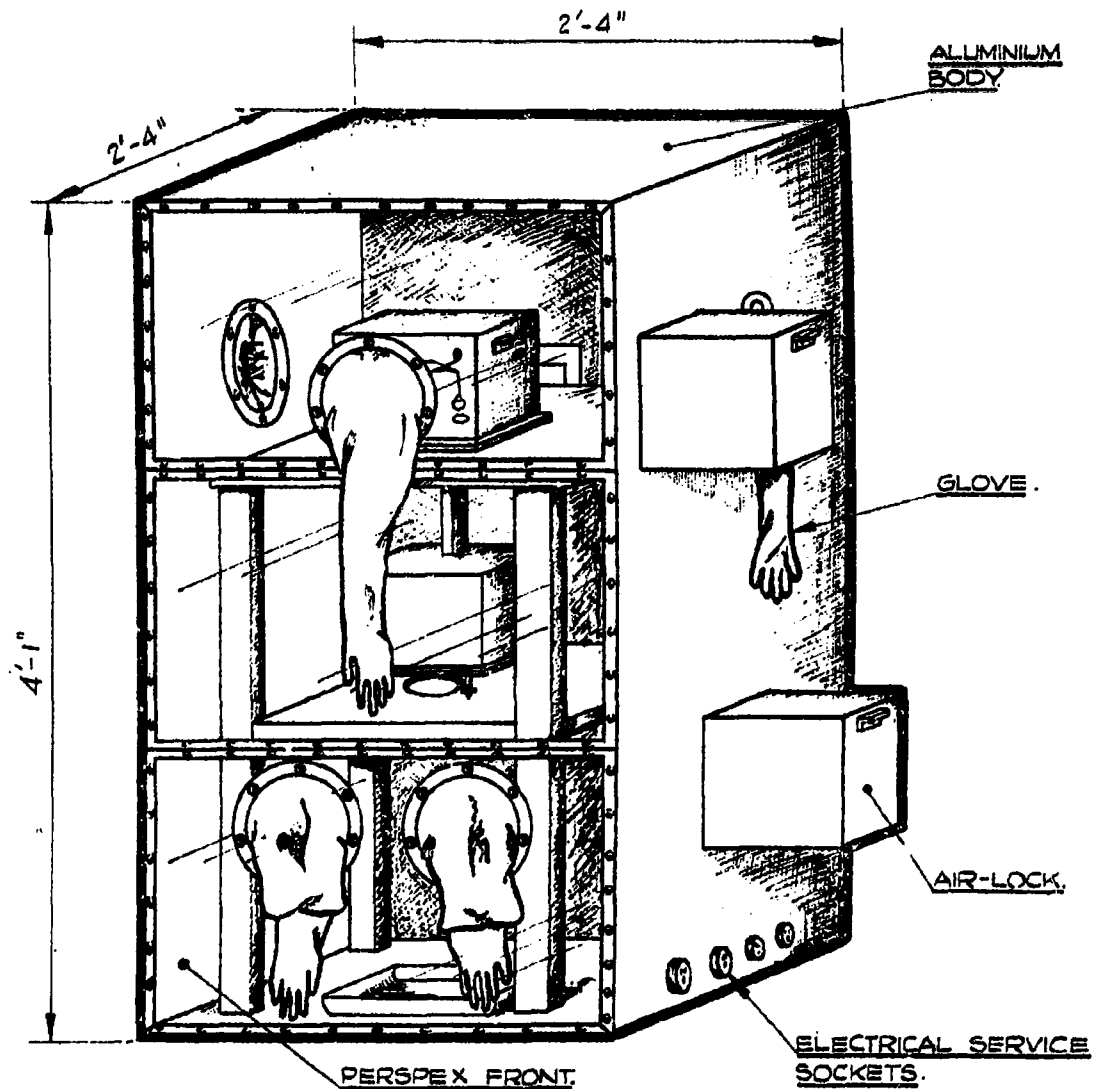


FIG. 4.



DRY-BOX USED TO HOUSE APPARATUS FOR LOW HUMIDITY STUDIES.

FIG. 5

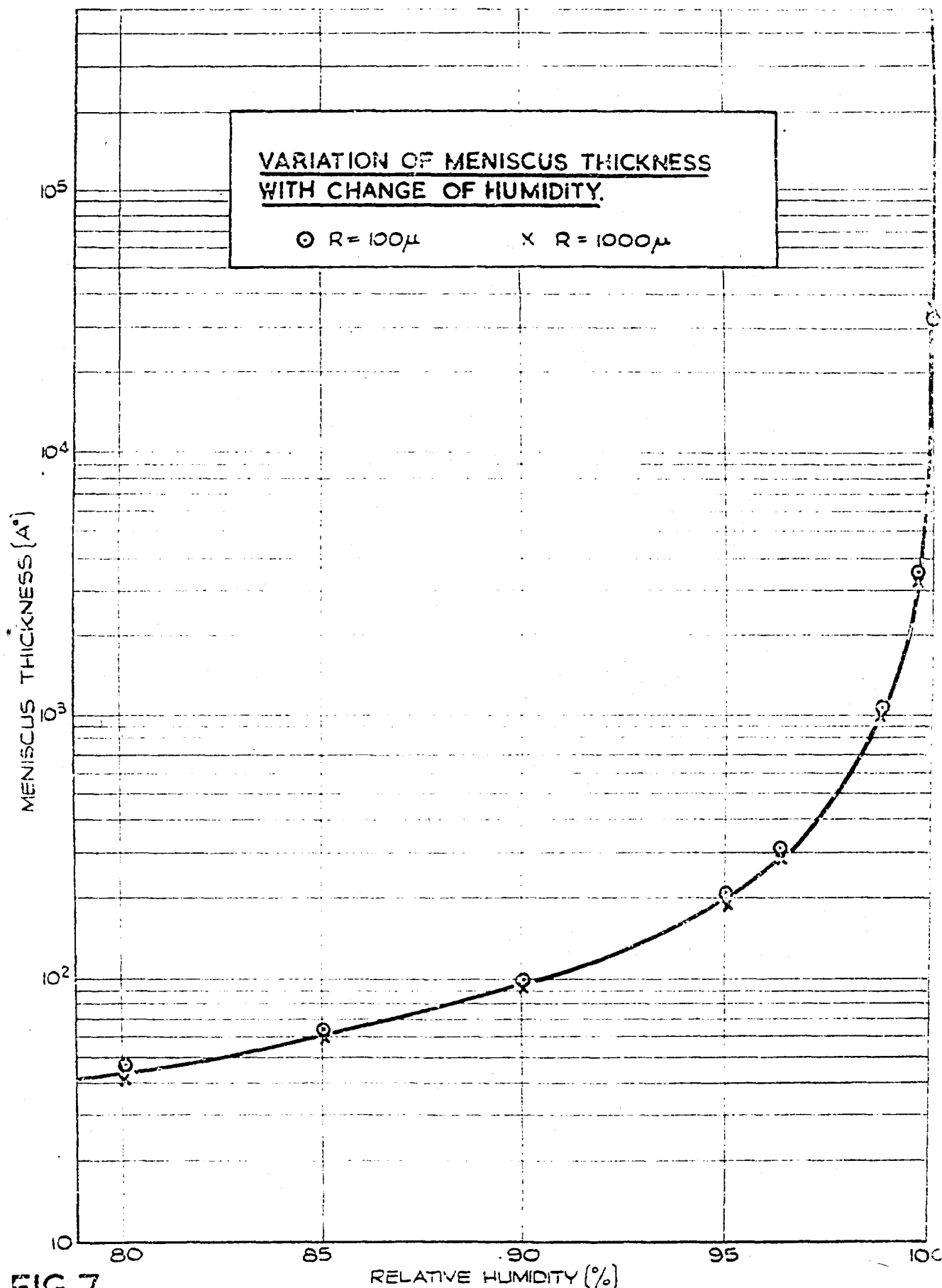
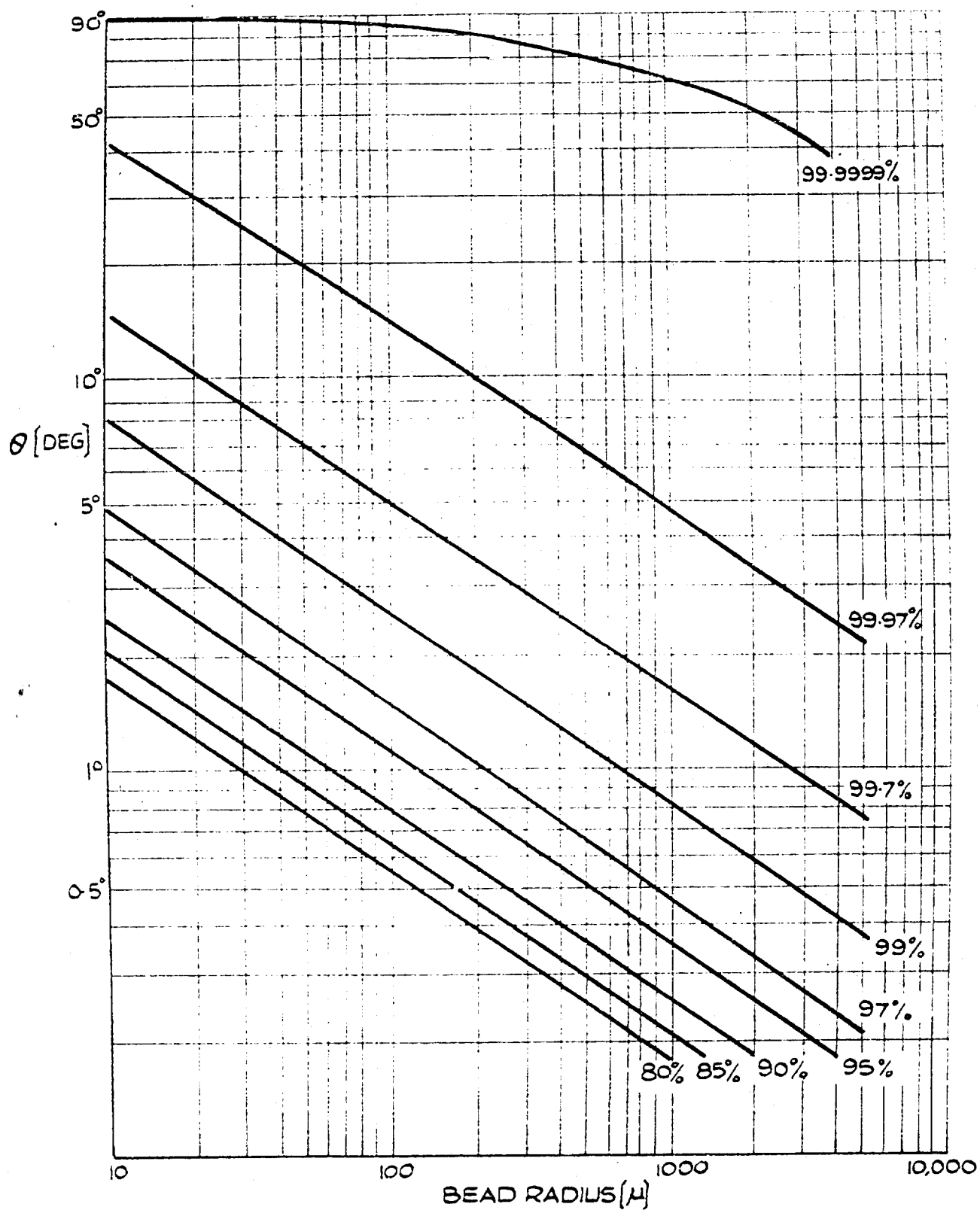


FIG. 7



VARIATION OF θ WITH BEAD RADIUS AT HIGH HUMIDITIES.

FIG. 8

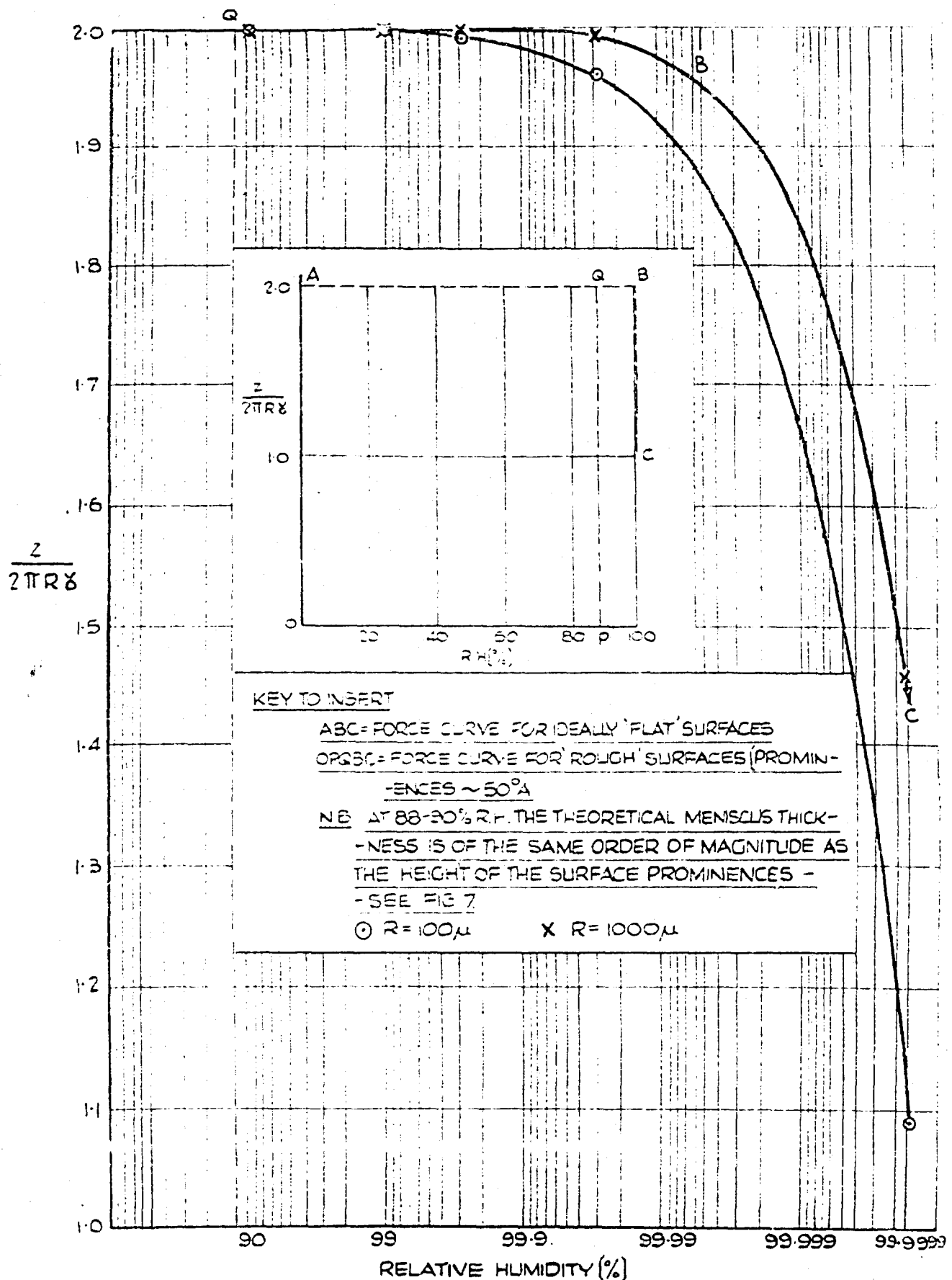
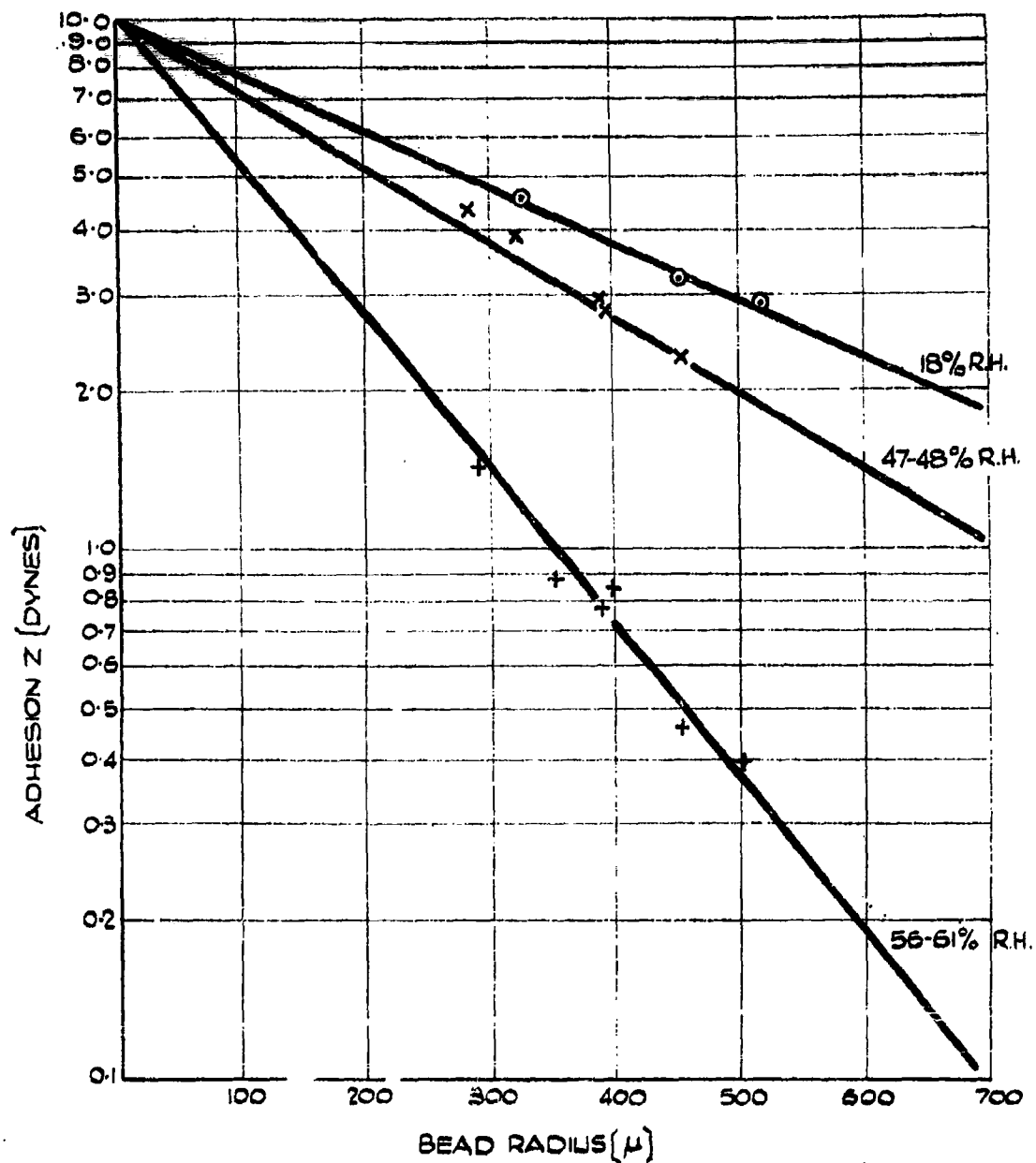


FIG.9

VARIATION OF SURFACE TENSIONAL FORCE (Z) WITH CHANGE IN HUMIDITY.

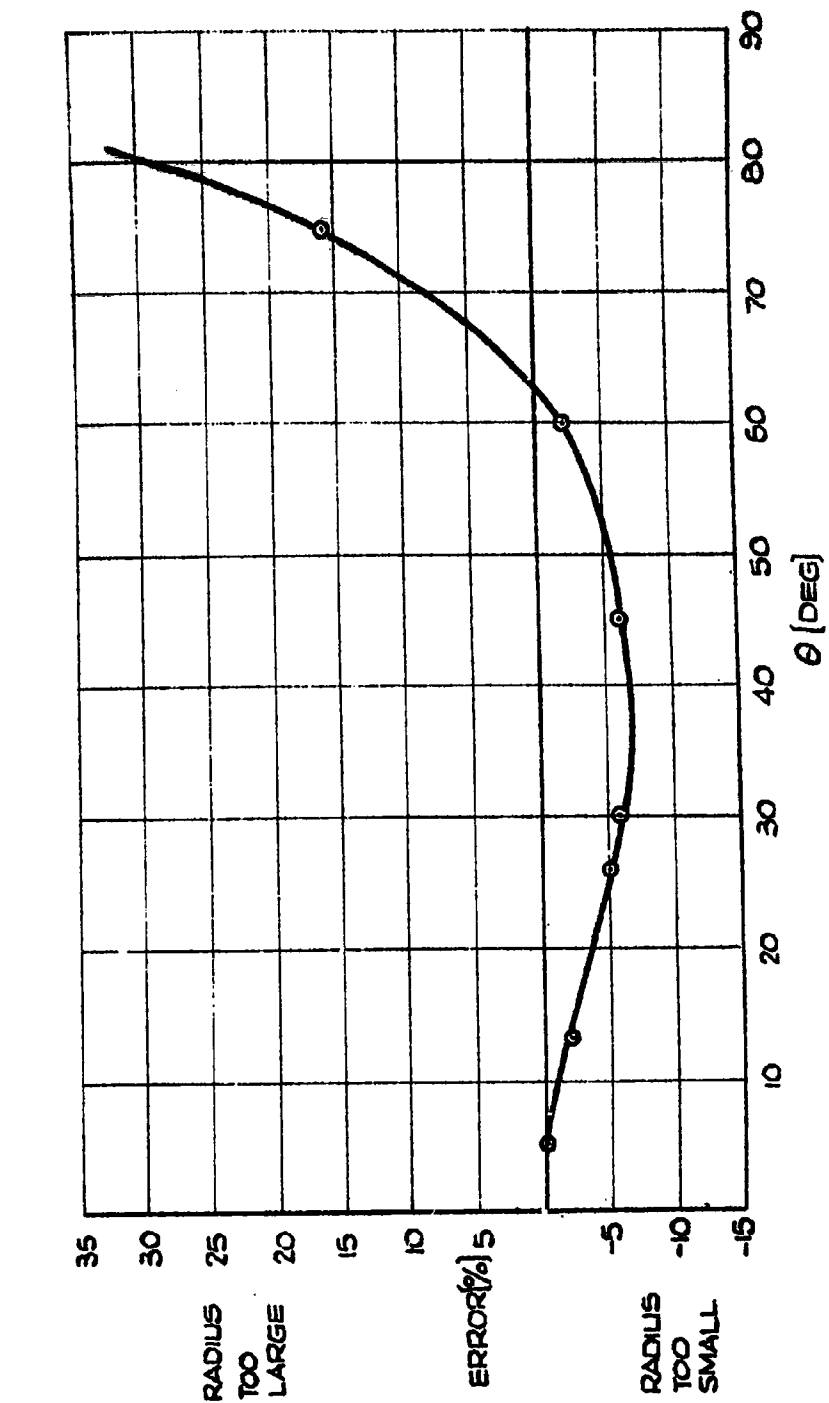


ADHESION OF RADIO-ACTIVE MICROSPHERES ON GLASS
AT VARIOUS HUMIDITIES.

FIG. 10.

PORTON TECHNICAL PAPER (R) 35.

PT. 3964

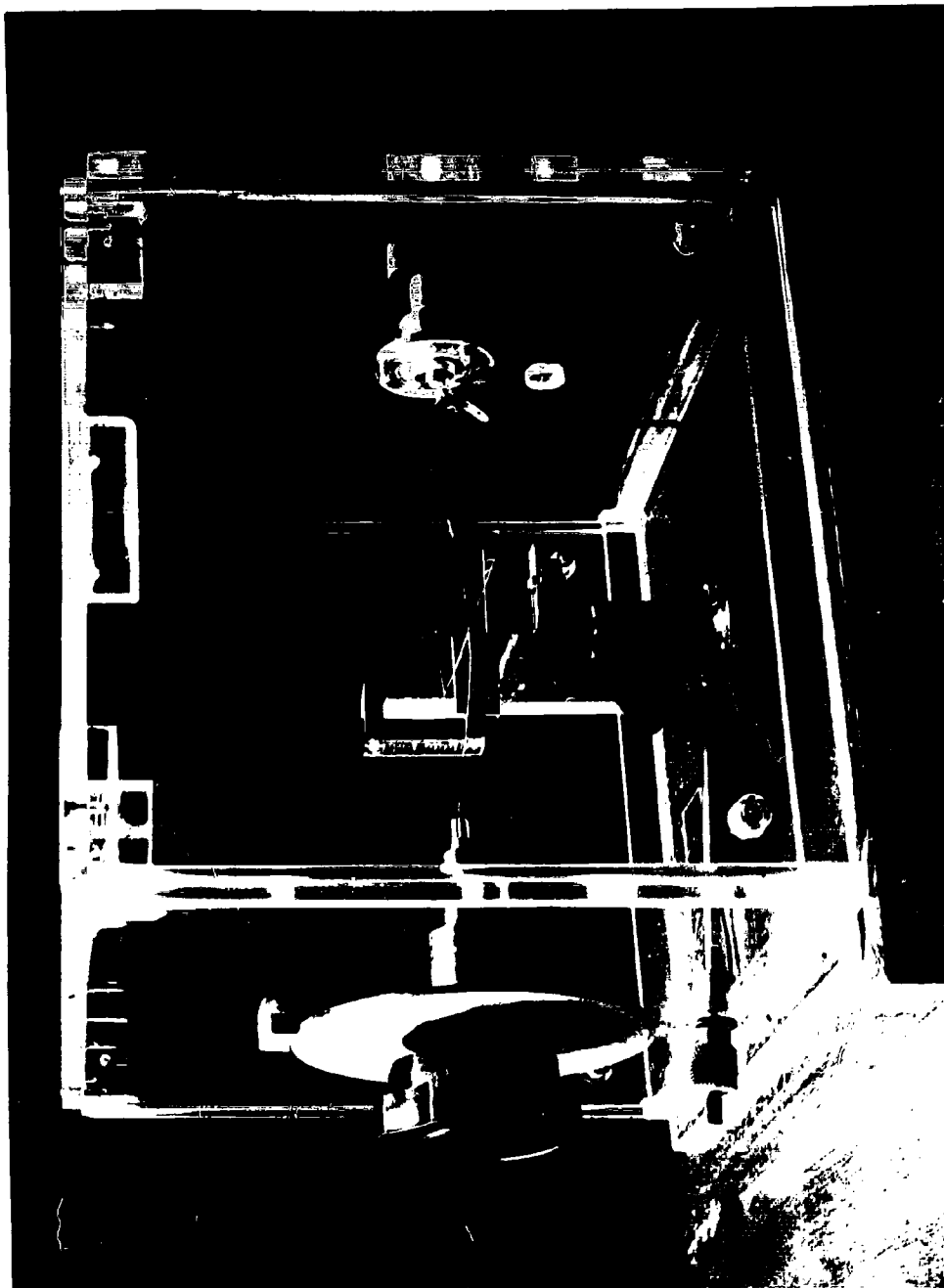


ERROR TAKING RADIUS OF OSCULATORY
CIRCLE INSTEAD OF CORRECT VALUE FOR $(r_1)_M$

FIG. 11

PORTON TECHNICAL PAPER (R) 35.

PT. 396



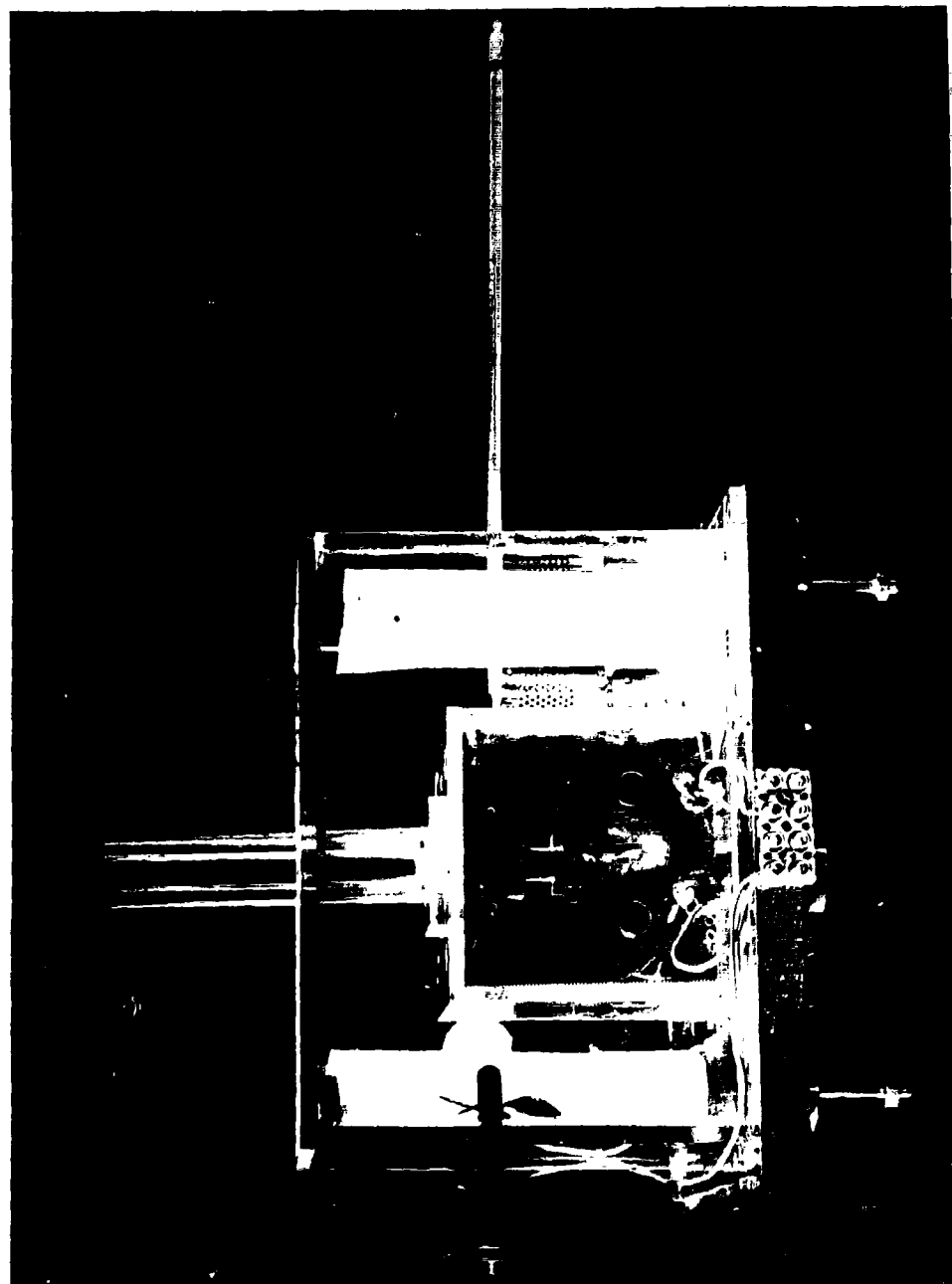
TORSION BALANCE.

FIG. 12.

L. 2285/2.

T.1685/1.

P.T.P. (R) 35.



HUMIDITY CHAMBER.

FIG. 13.

L. 2285/3.

T. 1685/2.

P.T.P. (R) 35.

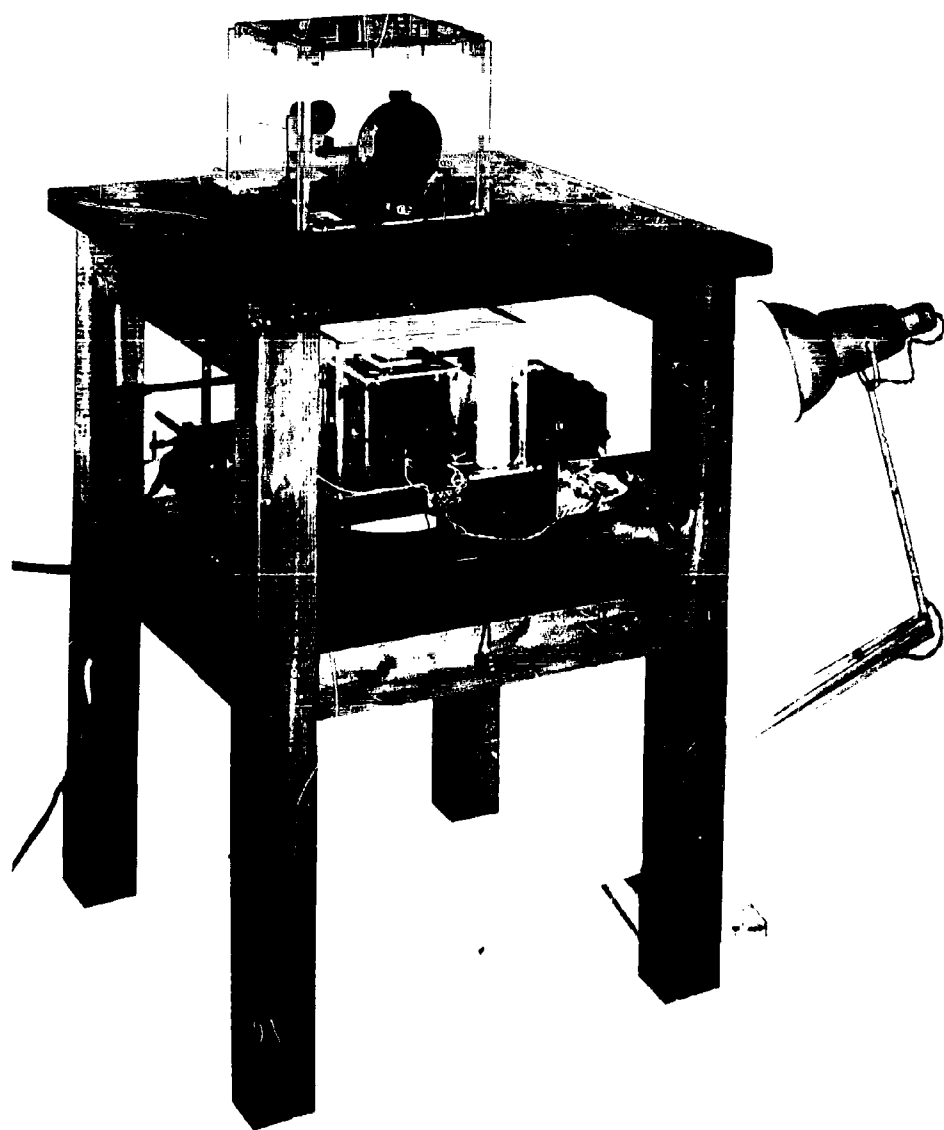


FIG. 14.

COMPLETE APPARATUS.

T. 1685/3.

P.T.P. (R) 35.

RESTRICTED

DISTRIBUTION

PORTON TECHNICAL PAPER NO. (R) 35

WAR OFFICE

D.C.S. (A)
D.C.D.R.D. (4 copies)
E.P.4.

R. & D. Establishments

C.D.E.E.
M.R.E.
W.O. Estab. Nancekuke (2 copies)

Advisory Bodies

Members of C.D.A.B. (10 copies)
Members of Physics and Physical
Chemistry Committee (8 copies)
Scientific Advisory
Council (8 copies)

AIR MINISTRY

D.G.D.

MINISTRY OF AVIATION

D.A.W. (Plans)
T.I.L. (2 copies)
D.R.A.E.

MINISTRY OF DEFENCE

Mr. V. H. B. Macklen

HOME OFFICE

C.S.A.'s Dept. (3 copies)
(1 copy attn. Dr. McAulay)

U.K. ATOMIC ENERGY AUTHORITY

D.A.E.R.E.
D.A.W.R.E.

BRITISH JOINT SERVICES MISSION

R. Holmes, Esq., D.R. Staff (1 copy)

OVERSEAS (through T.I.L.)

AUSTRALIA

Defence Research Laboratories (3 copies)
Senior Representative, Dept. of Supply
Army Branch Representative.
R.A.A.F. (Technical Section).

CANADA

Chairman, Defence Research Board (2 copies)
Defence Research Chemical Laboratories,
Ottawa (2 copies)
Suffield Experimental Station

U.S.A.

Reading Panel (13 copies)
U.S. Chem. Corps Liaison Officer, Porton
(7 copies)

RESTRICTED

CONFIDENTIAL
MODIFIED HANDLING AUTHORIZED

CONFIDENTIAL
MODIFIED HANDLING AUTHORIZED

**DEFENSE TECHNICAL INFORMATION CENTER
REQUEST FOR RELEASE OF LIMITED DOCUMENT**

DTIC CONTROL NO.

REQUEST ROUTING

3091007

8981U

SECTION I - REQUESTING ORGANIZATION

1. REQUESTING ORGANIZATION AND ADDRESS	2. DTIC USER CODE NO.	3. DATE OF REQUEST 3/11/03
TYPE COPY AND QUANTITY <input checked="" type="checkbox"/> Paper Copy <u>1</u> Copy(s) <input type="checkbox"/> Microfiche <u> </u> Copy(s)		
5. CONTRACT NUMBER		6. CONTRACT SECURITY LEVEL
7. GOVERNMENT SPONSOR AND ADDRESS (Contractors Only)	8. METHOD OF PAYMENT (X ONE) <input type="checkbox"/> VISA <input type="checkbox"/> MC <input type="checkbox"/> AMX <input checked="" type="checkbox"/> Charge to my NTIS Deposit Account No: <u> </u> <input type="checkbox"/> Bill My Organization to the Attention of: <u> </u>	
9. CONTRACT MONITOR AND TELEPHONE NUMBER (Contractors Only)	10. NAME, TITLE, PHONE NUMBER OF REQUESTING OFFICIAL	

Title: ADHESION OF SPHERICAL PARTICLES TO PLANE SURFACES

AD Number: AD0324812. Corporate Author: CHEMICAL DEFENCE

EXPERIMENTAL ESTABLISHMENT PORTON DOWN (ENGLAND).

Personal Author: CROSS, N.L. STRETCH, H.. Report Date: April 01, 1961.

Media: 1 Page(s). Distribution Code: 13 - U.S. GOVT. ONLY; NON-DOD

CONTROLLED. Source Code: 080450. From the Collection: TR42.

13. REQUESTER JUSTIFICATION (Explain need in detail)

The documents are needed to extract relevant data dealing with all aspects of chemical, biological and nuclear agents/weapons. This includes, but is not limited to protection, detection, decontamination, persistency, agent fate in various substrates, and dissemination. This information is to be used I support of CINPAC, CINCPACAF, CINCUSFK, CINCCENTCOM, and USAF Headquarters XONP.

SECTION IV - RELEASING AGENCY

1. RELEASING AGENCY ADDRESS (If Known)	2. RELEASING AGENCY DECISION (If the report was developed under the SBIR Program, refer to Instruction B.2)		
BRITISH MINISTRY OF AVIATION CHEM DEF EXPER ESTABLISHMENT PORTON DOWN ENGLAND, UK	<input type="checkbox"/> APPROVED FOR RELEASE TO THE ABOVE REQUESTOR <input type="checkbox"/> DISAPPROVED. REASON FOR DISAPPROVAL: <u> </u> <input checked="" type="checkbox"/> APPROVED FOR PUBLIC RELEASE <input type="checkbox"/> DISTRIBUTION AUTHORIZED TO U.S. GOVT AGENCIES & THEIR CONTRACTORS <input type="checkbox"/> DISTRIBUTION AUTHORIZED TO U.S. GOVT AGENCIES ONLY <input type="checkbox"/> DISTRIBUTION AUTHORIZED TO DOD ONLY <input type="checkbox"/> DISTRIBUTION AUTHORIZED TO DOD & THEIR CONTRACTORS		
	3. NAME AND TITLE OF RELEASING OFFICIAL	4. TELEPHONE NO.	5. SIGNATURE
	6. DATE		

DTIC FORM JUL 2000 55

Open publication is
available at Public Record
Office